Dalton Transactions

Accepted Manuscript



This is an *Accepted Manuscript*, which has been through the Royal Society of Chemistry peer review process and has been accepted for publication.

Accepted Manuscripts are published online shortly after acceptance, before technical editing, formatting and proof reading. Using this free service, authors can make their results available to the community, in citable form, before we publish the edited article. We will replace this Accepted Manuscript with the edited and formatted Advance Article as soon as it is available.

You can find more information about *Accepted Manuscripts* in the **Information for Authors**.

Please note that technical editing may introduce minor changes to the text and/or graphics, which may alter content. The journal's standard <u>Terms & Conditions</u> and the <u>Ethical guidelines</u> still apply. In no event shall the Royal Society of Chemistry be held responsible for any errors or omissions in this *Accepted Manuscript* or any consequences arising from the use of any information it contains.



Syntheses, structures, and optical properties of Ba₄Ga₄SnSe₁₂ and Ba₆Ga₂SnSe₁₁†

Wenlong Yin, Zuohong Lin, Elei Kang, Bin Kang, Jianguo Deng, Zheshuai Lin, Jiyong Yao, *Yicheng Wu

Two new quaternary selenides, namely $Ba_4Ga_4SnSe_{12}$ and $Ba_6Ga_2SnSe_{11}$, have been synthesized for the first time, representing the first two members in the A/M/Sn/Q (A = alkaline–earth metal; M = Al, Ga, In; Q = S, Se, Te) system. $Ba_4Ga_4SnSe_{12}$ crystallizes in the non–centrosymmetric space group $P\overline{4}\,2_1/c$ of the tetragonal system and has a three–dimensional structure. Its three–dimensional framework is built up from corner–sharing $GaSe_4$ and $SnSe_4$ tetrahedra with eight–coordinated Ba^{2+} cations residing in the cavities. $Ba_6Ga_2SnSe_{11}$ crystallizes in a new structure type in the monoclinic centrosymmetric space group $P2_1/c$. The structure of $Ba_6Ga_2SnSe_{11}$ features a zero–dimensional structure containing totally isolated distorted $SnSe_4$ tetrahedra and discrete Ga_2Se_7 unit with Ba^{2+} cations located between them. On the

^a Institute of Chemical Materials, China Academy of Engineering Physics, P.O. Box 919-306 Mianyang, 621900, China,

^b Key Laboratory of Functional Crystals and Laser Technology, Technical Institute of Physics and Chemistry, Chinese Academy of Sciences, Beijing 100190, China, Email: jyao@mail.ipc.ac.cn

^cUniversity of the Chinese Academy of Sciences, Beijing 100049, China,

[†]Electronic supplementary information (ESI) available: Crystallographic data in CIF format for Ba₄Ga₄SnSe₁₂ and Ba₆Ga₂SnSe₁₁.

basis of the diffuse–reflectance spectra, the band gaps are 2.16 (2) eV and 1.99 (2) eV for $Ba_4Ga_4SnSe_{12}$ and $Ba_6Ga_2SnSe_{11}$ respectively. In addition, electronic structure calculation on $Ba_4Ga_4SnSe_{12}$ indicates that it is a direct–gap semiconductor with the band gap mainly determined by the $[Ga_4SnSe_{12}]^{8-}$ anionic framework.

Introduction

Over the past decades, the chalcogenide semiconductors possessing multi-cations have received increased attention for their amazing structural and compositional complexity and fascinating physical properties including magnetic, superconducting, thermoelectric, electrical, and nonlinear optical properties. ¹⁻³⁶ For example, the new layered compound CsHgInS₃ has a γ-ray attenuation length comparable to commercial Cd_{1-x}Zn_xTe showing promising properties for X-ray and γ-ray detection;¹ Bi-Bi bonds containing compound CsBi₄Te₆ exhibits attractive thermoelectric properties with a thermoelectric figure of merit $\Box 0.8$ at the temperature 225 K when doped appropriately; ALnMQ₃ (A = Rb, Cs; Ln = rare-earth metal; M = Mn, Co, Zn, Cd, Hg; Q = S, Se, Te) offer flexibility in band gap engineering by controlling the composition and crystal orientation;³⁻⁷ Ba₈Hg₃U₃S₁₈ contains interesting infinite chains of US₆ octahedra and nearly linear [S-Hg-S]²⁻ dithiomercurate anions; 8 Cs₅BiP₄Se₁₂, 9 Rb₃Ta₂AsS₁₁, 10 La₄InSbS₉, 11 Sm₄GaSbS₉, 12 LiAsS₂,¹³ and γ-NaAsSe₂¹⁴ exhibit very strong second harmonic generation (SHG) responses in the IR range indicating their potential use in laser frequency conversion applications; copper–based quaternary chalcopyrite semiconductors Cu₂ZnMQ₄ (N = Ge, Sn; Q = S, Se) have large photoelectric responses, indicating that they are promising candidates for photovoltaic applications. 15–17

In one of our earlier studies, we explored the quaternary A/M/M'/Q (A = alkaline-earth metal; M = Al, Ga, In; M' = Si, Ge; Q = S, Se, Te) system and found

four isostructural compounds BaGa₂MQ₆ (M = Si, Ge; Q = S, Se) which were characterized as a new series of IR nonlinear optical materials promising for practical applications.³⁷ These results inspire us to make further efforts to synthesize new compounds in related system. In this paper, by focusing on the heavier group 14 element Sn instead of the lighter Si and Ge elements, we extend our study to the A/M/Sn/Q (A = alkaline-earth metal; M = Al, Ga, In; Q = S, Se, Te) system. Sn atom can be stabilized in both at a +2 oxidation state with an electron lone pair and a +4 oxidation state typically in a tetrahedral environment in chalcogenides, the mixed valence property of Sn will increase the diversity in their stoichiometry and structure. For example, Ba₆Sn₆Se₁₃ has mixed valent Sn²⁺/Sn⁴⁺ atoms with 3-fold, 4-fold and 5-fold coordinated Sn atoms simultaneously and demonstrates modest IR NLO response.³⁸ Moreover, comparing with the large number (almost 80) of ternary chalcogenides in A/M/Q (A = alkaline–earth metal; M = Al, Ga, In; Q = S, Se, Te) and Sn/M/Q (M = Al, Ga, In; Q = S, Se, Te) system, there is surprisingly no compound reported in the A/M/Sn/Q (A' = alkaline-earth metal; M = Al, Ga, In; Q = S, Se, Te) system. The combination of metal cations with different bonding nature, formal charge, and size would greatly increase the diversity of stoichiometry and structure of new compound and may lead to interesting physical properties. Here, our detailed exploratory investigation has led to the discovery of two new selenides Ba₄Ga₄SnSe₁₂ and Ba₆Ga₂SnSe₁₁ representing the first two numbers in the A/M/Sn/Q system. This work presents the syntheses, structural characterizations, and experimentally determined band gaps of Ba₄Ga₄SnSe₁₂ and Ba₆Ga₂SnSe₁₁ as well as the electronic

band structure of Ba₄Ga₄SnSe₁₂.

Experimental Section

Syntheses

The following reagents were used as obtained: Ba (Aladdin Co., Ltd., 99%), Ga (Sinopharm Chemical Reagent Co., Ltd., 99.99%), Sn (Sinopharm Chemical Reagent Co., Ltd., 99.99%), and Se (Sinopharm Chemical Reagent Co., Ltd., 99.95%). The binary starting materials, BaSe, Ga_2Se_3 , and $SnSe_2$ were synthesized by the stoichiometric reactions of elements at high temperatures (850 °C for BaSe, 900 °C for Ga_2Se_3 , 600 °C for $SnSe_2$) in sealed silica tubes evacuated to 10^{-3} Pa. The ternary starting material $SnGa_4Se_7$ was synthesized by the stoichiometric reaction of the binary materials in the molar ratio of SnSe: $Ga_2Se_3 = 1:2$ at high temperature in sealed silica tube evacuated to 10^{-3} Pa.

Ba₄Ga₄SnSe₁₂. Crystals of Ba₄Ga₄SnSe₁₂ were initially obtained from a reaction between BaSe and SnGa₄Se₇ in the molar ratio of 4:1. The mixture of 112 mg BaSe and 124 mg SnGa₄Se₇ was ground and loaded into a fused–silica tube under an Ar atmosphere in a glovebox. The tube was flame-sealed under a high vacuum of 10⁻³ Pa and then placed in a computer–controlled furnace. The reaction mixture was heated to 950 °C in 15 h, kept at 950 °C for 48 h, followed by slow cooling to 320 °C at a rate of 3 °C/h, and finally cooled to room temperature by switching off the furnace. Many orange block–shaped crystals, subsequently determined as Ba₄Ga₄SnSe₁₂, were found in the ampule. The SEM picture of as–grown Ba₄Ga₄SnSe₁₂ crystal is shown in

Fig. 1. Analyses of the crystals with an EDX-equipped Hitachi S-4800 SEM showed the presence of Ba, Ga, Sn, and Se in the approximate ratio of 4:4:1:12. The crystals are stable in air.

Ba₆Ga₂SnSe₁₁. Crystals of Ba₆Ga₂SnSe₁₁ were initially obtained from a reaction between BaSe and SnGa₄Se₇ in the molar ratio of 5:1. The mixture (BaSe 108 mg, SnGa₄Se₇ 95 mg) was ground and loaded into a fused–silica tube under an Ar atmosphere in a glovebox. The tube was flame–sealed under a high vacuum of 10⁻³ Pa and then placed in a computer–controlled furnace. The reaction mixture was heated to 950 °C in 15 h, kept at 950 °C for 48 h, followed by slow cooling to 320 °C at a rate of 3 °C/h, and finally cooled to room temperature by switching off the furnace. Many orange block–shaped crystals (as shown in Fig. 2), subsequently determined as Ba₆Ga₂SnSe₁₁, were found in the ampule. Analyses of the crystals with an EDX–equipped Hitachi S–4800 SEM showed the presence of Ba, Ga, Sn, and Se in the approximate ratio of 6:2:1:11. The crystals are stable in air.

Based on the single crystal crystallographic study and EDX measurement, the composition of the crystals were determined as Ba₄Ga₄SnSe₁₂ and Ba₆Ga₂SnSe₁₁. Then the stoichiometric syntheses of Ba₄Ga₄SnSe₁₂ and Ba₆Ga₂SnSe₁₁ polycrystalline samples were carried out using reactions shown in the following equations:

$$4 BaSe + 2 Ga2Se3 + SnSe2 \rightarrow Ba4Ga4SnSe12$$

$$6\;BaSe+Ga_2Se_3+SnSe_2{\longrightarrow}Ba_6Ga_2SnSe_{11}$$

The mixtures of BaSe, Ga₂Se₃, and SnSe₂ in the molar ratio of 4:2:1 (BaSe 865 mg, 4 mmol; Ga₂Se₃ 753 mg, 2 mmol; SnSe₂ 277 mg, 1 mmol) and 6:1:1(BaSe 1298

mg, 6 mmol; Ga_2Se_3 376 mg, 1 mmol; $SnSe_2$ 277 mg, 1 mmol) for $Ba_4Ga_4SnSe_{12}$ and $Ba_6Ga_2SnSe_{11}$ respectively were ground and loaded into fused–silica tubes under an Ar atmosphere in a glovebox. The tubes were sealed under 10^{-3} Pa atmosphere and then placed in a computer–controlled furnace. The samples were heated to 800 °C in 15 h, kept at that temperature for 48 h, and then the furnace was turned off.

X-ray Powder Diffraction

X–ray powder diffraction of the resultant powder samples were performed at room temperature in the angular range of $2\theta = 10$ – 70° with a scan step width of 0.02° and a fixed counting time of 0.1 s/step using an automated Bruker D8 X–ray diffractometer equipped with a diffracted monochromator set for Cu K_{\alpha} ($\lambda = 1.5418$ Å) radiation. The experimental powder X–ray diffraction patterns were found to be in good agreement with the calculated ones based on the single crystal crystallographic data (Figs. 3 and 4).

Structure Determination

The single crystal X–ray diffraction measurement was performed on a Rigaku AFC10 diffractometer equipped with a graphite–monochromated K_{α} (λ = 0.71073 Å) radiation at 153 K. The Crystalclear software³⁹ was used for data extraction and integration and the program XPREP⁴⁰ was used for face–indexed absorption corrections.

The structure was solved with Direct Methods implemented in the program SHELXS and refined with the least–squares program SHELXL of the SHELXTL.PC suite of programs.⁴⁰ The final refinement included anisotropic displacement parameters and a secondary extinction correction. Additional experimental details are given in Table 1 and selected metrical data are given in Tables 2 and 3. Further information may be found in the Electronic supplementary information.

Diffuse Reflectance Spectroscopy

A Cary 1E UV-visible spectrophotometer with a diffuse reflectance accessory was used to measure the spectra of Ba₄Ga₄SnSe₁₂ and Ba₆Ga₂SnSe₁₁ in the range of 300 nm (4.13 eV) to 2500 nm (0.496 eV). The optical absorption spectra were converted from diffuse–reflectance spectra using the Kubelka–Munk function, $a/S = (1-R)^2/2R$, where a is the Kubelka–Munk absorption coefficient and S is the scattering coefficient.

Second-Harmonic Generation Measurement

Optical second–harmonic generation (SHG) test of Ba₄Ga₄SnSe₁₂ was performed by means of the Kurtz–Perry method. Fundamental 2090 nm light was generated with a Q-switched Ho:Tm:Cr:YAG laser. The particle sizes of the sieved samples are 80–100 µm. Microcrystalline AgGaS₂ of similar particle size served as reference.

Theoretical Calculation

The first–principles calculations at the atomic level for the Ba₄SnGa₄Se₁₂ crystal, including the band structure, total/partial density of states (DOS/PDOS) are performed by the plane—wave pseudopotential method⁴¹ implemented in the CASTEP program⁴² based on density functional theory (DFT).⁴³ The exchange–correlation (XC) functionals is described by the local density approximation (LDA).⁴⁴ The ion–electron interactions are modeled by the ultrasoft pseudopotentials⁴⁵ for all constituent elements. In this model, Ba 5s²5p⁶6s², Sn 5s²5p², Se 4s²4p⁴, and Ga 3d¹⁰4s²4p¹ electrons are treated as the valence electrons, respectively. The ultra–fine kinetic energy cutoff of 330 eV and Monkhorst–Pack *k*–point meshes⁴⁶ spanning less than 0.04/Å³ in the Brillouin zone are chosen to ensure the sufficient accuracy of the present purposes.

Results and Discussion

Syntheses

The crystals of two new quaternary selenides Ba₄Ga₄SnSe₁₂ and Ba₆Ga₂SnSe₁₁ have been obtained from the reactions of BaSe and SnGa₄Se₇ by traditional high-temperature solid state reactions for the first time with the starting materials BaSe and SnGa₄Se₇ in the molar ratio of 4:1 and 5:1, respectively. The valence state of Sn atom in the ternary raw material SnGa₄Se₇ is +2, however in the title products Ba₄Ga₄SnSe₁₂ and Ba₆Ga₂SnSe₁₁; the oxidation state of +4 is attributed to Sn atom. Clearly, the introduction of strongly ionic Ba atom to the Sn/Ga/Se system could increase the valence of atoms which are under low oxidation state. The similar

phenomenon has been observed in the compound $Ba_5Ga_4Se_{10}$ containing Ga in the 2+/3+ valence states, which were obtained from the reaction of BaSe and GaSe in the molar ratio of 1:1 at high temperature.⁴⁷

Structures

Ba₄**Ga**₄**SnSe**₁₂. The compound Ba₄Ga₄SnSe₁₂ has been obtained for the first time, it crystallizes in the Pb₄Ga₄GeSe₁₂—related structure type¹⁹ in the non–centrosymmetric space group $P\overline{4}$ 2₁/c of the tetragonal system with a = 13.607 (2) Å, c = 6.510(2) Å, and Z = 2. In the asymmetric unit, there are one crystallographically unique Ba atom, one Ga atom, one Sn atom, and three Se atoms. The Sn atom lies in the Wyckoff position 2b with $\overline{4}$ axis symmetry, while all other atoms lie at general positions 8e.

The structure of Ba₄Ga₄SnSe₁₂ is illustrated in Fig. 5. It features a three–dimensional structure built up from corner–sharing GaSe₄ and SnSe₄ tetrahedra with eight–coordinated charge–compensating Ba²⁺ cations residing in the cavities. The GaSe₄ tetrahedra are slightly distorted with Ga–Se distances ranging from 2.387 to 2.451 Å (as shown in Table 2) and Se–Ga–Se angles varying from 100.72 to 116.07°. The SnSe₄ tetrahedra are slightly distorted with Sn–Se bond lengths of 2.438 Å and Se–Sn–Se angles of 96.55 and 116.30°. These bond lengths and angles agree well with the values for related compounds, such as 2.362–2.427 Å and 101.54–114.11° in Ba₄LiGa₅Se₁₂⁴⁸ and 2.508–2.554 Å and 98.41–115.30° in Ba₆Sn₆Se₁₃.³⁸ In the structure, the distorted GaSe₄ tetrahedra are connected by corner–sharing to form zigzag [GaSe₃]³⁻ chains along the *c* direction and these chains

are further connected by the separated SnSe₄ tetrahedra to form [Ga₂SnSe₁₀]¹⁰⁻ layers parallel to the (110) plane (Fig. 6). These layers are then joined together via GaSe₄ tetrahedra along the [110] direction forming a three–dimensional framework with channels along the *c* direction occupied by the Ba atoms (Fig. 5). In Ba₄Ga₄SnSe₁₂, the calculated band valence sums (BVS)⁴⁹ are 2.043, 2.939, and 4.860 for Ba, Ga, and Sn respectively (as shown in Table 4), which are close to the expected values of +2 for Ba, +3 for Ga, and +4 for Sn. Considering the bonding in the structure, the oxidation states of 2+, 3+, 4+, and 2- can be attributed to Ba, Ga, Sn, and Se, respectively and in this way charge balance can be achieved.

Although Ba₄Ga₄SnSe₁₂ adopts a structure closely related to the Pb₄Ga₄GeSe₁₂, the bivalent Pb atoms in Pb₄Ga₄GeSe₁₂ are coordinated to seven Se atoms with the Pb–Se distances ranging from 2.90 (4) to 3.55 (4) Å. In contrast, Ba ions in Ba₄Ga₄SnSe₁₂ are coordinated to eight Se atoms in a more "sphere" environment with the Ba–Se distances ranging from 3.29 (4) to 3.65 (4) Å. The larger difference in the Pb–Se distances results from the steorochemical activity of the 6s² lone pair of electron of Pb. Another compound that has the same space group and similar structure with Ba₄Ga₄SnSe₁₂ is Ba₄Ga₅LiSe₁₂ and the structure difference between them is that the zigzag [GaSe₃]³⁻ chains in Ba₄LiGa₅Se₁₂ are connected by another kind of chains formed by alternately arranged edge–sharing GaSe₄ and LiSe₄ tetrahedra (Fig. 7) while the [GaSe₃]³⁻ chains in Ba₄Ga₄SnSe₁₂ are connected by the separated SnSe₄ tetrahedra only.

Ba₆Ga₂SnSe₁₁. The compound Ba₆Ga₂SnSe₁₁ has been obtained for the first time,

it crystallizes in a new structure type in the centrosymmetric space group $P2_1/c$ of the monoclinic system with unit cell permanents of a = 18.715 (4) Å, b = 7.109 (1) Å, c =19.165 (4) Å, $\beta = 103.29$ (3) °, and Z = 4. The asymmetric unit contains six crystallographically independent Ba atoms, two Ga atoms, and eleven Se atoms, while the Sn atoms at disordered at two adjacent positions with 80.6 % and 19.4 % occupancy respectively. All atoms lie at general positions 4e. The Ga and Sn atoms are coordinated to a distorted tetrahedron of four Se atoms with Ga-Se distances ranging from 2.358 (1) to 2.496 (1) Å and Sn-Se distances ranging from 2.479 (5) to 2.968 (7) Å which are comparable to the Ga-Se and Sn-Se bond length observed in $BaGa_4Se_7\ (2.361\ to\ 2.488\ \mbox{\normalfont\AA}\ for\ Ga-Se)^{50}\ and\ Ba_6Sn_6Se_{13}\ (2.508\ to\ 3.268\ \mbox{\normalfont\AA}\ for$ Sn-Se)³⁵ respectively, while the Ba atoms have three different kinds of coordination geometry. The Ba1, Ba3, Ba4, and Ba5 atoms are eight-coordinated to Se atoms in a distorted bicapped trigonal prismatic geometry with the Ba-Se distances ranging from 3.166 (1) to 3.775 (1) Å, which are in agreement with those of 3.244 to 3.801 Å in Ba₂InErSe₅;²⁸ while the Ba2 atoms are coordinated with nine Se atoms in a distorted tricapped trigonal prismatic geometry with the Ba–Se distances ranging from 3.266(1) to 3.746(1) Å, which are close to those in BaLaSb₂Se₆ (3.2604 to 3.8079 Å);⁵¹ whereas the Ba6 atoms are coordinated to a distorted monocapped trigonal prism of seven Se atoms with the Ba-Se distances ranging from 3.110(1) to 3.582(1) Å, which are comparable to those of 3.228 to 3.769 Å in Ba₆Sn₆Se₁₃. The BVS for Ba, Ga, and Sn in Ba₄Ga₄SnSe₁₂ are shown in Table 4, which are close to the expected values of +2 for Ba, +3 for Ga, and +4 for Sn. Considering the bonding in the structure, the

oxidation states of 2+, 3+, 4+, and 2- can be attributed to Ba, Ga, Sn, and Se, respectively and in this way charge balance can be achieved.

The structure of Ba₆Ga₂SnSe₁₁ is displayed in Fig. 8. The compound features a zero-dimensional structure containing totally isolated distorted SnSe₄ tetrahedra and discrete Ga₂Se₇ unit formed by a pair of distorted corner-sharing GaSe₄ tetrahedra with charge-compensating Ba²⁺ cations located between them. As stated earlier, there are no quaternary compounds reported in A/M/Sn/Q (A = alkaline-earth metal; M = Al, Ga, In; Q = S, Se, Te) system before. In the ternary A/Ga/Se (A = Ba or Sn) system, six compounds, namely BaGa₄Se₇, ⁵⁰ BaGa₂Se₄, ⁵² Ba₅Ga₄Se₁₀, ⁴⁷ Ba₅Ga₂Se₈, ⁵³ SnGaSe2, 54 and SnGa4Se7 have been reported. The connectivity of the Ga-Se sublattice changes from simple isolated GaSe₄ tetrahedra in Ba₅Ga₂Se₈ to complex anion of [Ga₄Se₁₀]¹⁰⁻ in Ba₅Ga₄Se₁₀, to one-dimensional chain in BaGa₂Se₄, then to three-dimensional framework in BaGa₄Se₇, SnGaSe₂, and SnGa₄Se₇. Here, the quaternary Ba₆Ga₂SnSe₁₁ represents a new structure motif of discrete Ga₂Se₇ formed by a pair of distorted corner-sharing GaSe₄ tetrahedra. These structure types demonstrate the diversity in the connectivity and bonding of gallium compounds.

The selected bond distances for Ba₄Ga₄SnSe₁₂ and Ba₆Ga₂SnSe₁₁ are displayed in Tables 2 and 3. From above discussion and comparison with other compounds, it is evident that all the bond lengths in the title compounds are normal and common for BaSe₇ monocapped trigonal prism, BaSe₈ bicapped trigonal prism, BaSe₉ tricapped trigonal prism, GaSe₄ tetrahedra, and SnSe₄ tetrahedra respectively.

Experimental Band Gap

The optical absorption spectra converted from the Kubelka–Munk equation for Ba₄Ga₄SnSe₁₂ and Ba₆Ga₂SnSe₁₁ are shown in Fig. 9. The absorption edges of 574 nm and 624 nm for Ba₄Ga₄SnSe₁₂ and Ba₆Ga₂SnSe₁₁ respectively, and consequently optical band gaps of 2.16 (2) eV and 1.99 (2) eV were deduced with the use of the straightforward extrapolation method. The band gaps are consistent with the color of the materials. As discussed in the below Electronic Structure Calculations part, the Ba orbitals have negligible contribution to the bands around the Fermi level and the band gap is mainly determined by [GaSe₄]⁵⁻ and [SnSe₄]⁵⁻ anionic units. With the increasing ratio of Ga/Sn in the Ba/Ga/Sn/Se system, the GaSe₄ tetrahedra have more contribution to the bands around the Fermi level, leading to a larger band gap, as demonstrated in these two compounds Ba₄Ga₄SnSe₁₂ and Ba₆Ga₂SnSe₁₁.

Second-Harmonic Generation Measurement

With the use of the 2090 nm laser as the fundamental wavelength, the SHG property of the $Ba_4Ga_4SnSe_{12}$ compound was measured. Unfortunately, no obvious SHG signals were detected. As for the structure–related compounds $Pb_4Ga_4GeQ_{12}$ (Q = S, Se), the selenide $Pb_4Ga_4GeSe_{12}$ has a second harmonic generation (SHG) effect two times more efficient than the commercial $AgGaS_2$ at a particle size of 30–46 μ m, while the SHG effect on the sulfide $Pb_4Ga_4GeS_{12}$ at a fundamental laser radiation of 2.05 μ m is not observed. The packing of $GaSe_4$ and $SnSe_4$ tetrahedra in $Ba_4Ga_4SnSe_{12}$ is nearly the same as that of the $GaSe_4$ and $GeSe_4$ tetrahedra in $Pb_4Ga_4GeSe_{12}$, their

obvious difference in the nonlinear optical properties is amazing and may provide valuable information for exploring the mechanism of the nonlinear optical properties of chalcogenides. The mechanism of these different performances needs further investigation.

Theoretical Results

The electronic band structure of the Ba₄SnGa₄Se₁₂ in the unit cell is plotted along the symmetry lines in Fig. 10 (a). It is shown that Ba₄SnGa₄Se₁₂ is a direct gap crystal with calculated band gap of 1.42 eV, which is smaller than the experimental value (~ 2.16 eV). Due to the DFT calculations with the exchange–correlation (XC) functional of LDA, the band gap calculated is usually smaller than experimental value. The corresponding DOS/PDOS projected on the constitutional atoms is displayed in Fig. 10 (b). It is clear that the energy band is divided into two regions, i.e., valence band (VB) and conduction band (CB). The energy region below -5 eV is mainly composed of the isolated inner orbitals of Ba (5s) (5p), Sn (5s), Se (4s) and Ga (3d) (4s), which are strongly localized deep in the VB and have a negligible influence on electronic states close to the band gap. The top of the VB is mainly occupied by the p orbitals of Ga (4p) and Se (4p), and and the bottom of CB is mainly composed by the orbitals of Ga (4s) (4p) and Se (4s) (4p). The orbitals of Sn (5s) (5p) also contribute the near-region of band gap in some degree. It should be emphasized that the states on both sides of the band gap are mainly composed of the orbitals from the [GaSe₄]⁵⁻ groups and secondarily from the [SnSe₄]⁵⁻ groups. Since the optical response of a

crystal in the visible–IR region originates mainly from the electronic transitions between the VB and CB states close to the band gap,⁵⁶ the [GaSe₄]^{5–} and [SnSe₄]^{5–} anionic units mainly determine the optical properties of the Ba₄SnGa₄Se₁₂ crystal. Ba₄Ga₄SnSe₁₂ has a direct band gap mainly determined by the orbitals from Ga, Sn, and Se, while the closely–related Pb4Ga₄GeSe₁₂ possess an indirect band gap. These results clearly demonstrated the complexity of the properties of chalcogenides.

Conclusions

In summary, the two new compounds $Ba_4Ga_4SnSe_{12}$ and $Ba_6Ga_2SnSe_{11}$ represent the first two numbers in the quaternary A/M/Sn/Q (A = alkaline–earth metal; M = group 13 element Ga, In; Q = S, Se, Te) system. $Ba_4Ga_4SnSe_{12}$ crystallizes in the noncentrosymmetric space group $P\overline{4}\,2_1/c$ and has a three–dimensional framework which was built up from corner–sharing $GaSe_4$ and $SnSe_4$ tetrahedra with charge–compensating eight–coordinated Ba^{2+} cations located between them, meanwhile, $Ba_6Ga_2SnSe_{11}$ crystallizes in a new structure type in the centrosymmetric space group $P2_1/c$ of the monoclinic system with a zero–dimensional structure containing totally isolated distorted $SnSe_4$ tetrahedra and discrete Ga_2Se_7 unit. The novel discrete anionic Ga_2Se_7 unit in $Ba_6Ga_2SnSe_{11}$ formed by a pair of distorted corner–shared $GaSe_4$ tetrahedra is observed for the first time in compounds containing A/Ga/Se (A = alkaline–earth metal Ba or group 16 element Sn). As deduced from the diffuse reflectance spectra, the optical band gaps were 2.16 (2) eV and 1.99 (2) eV for $Ba_4Ga_4SnSe_{12}$ and $Ba_6Ga_2SnSe_{11}$ respectively. Furthermore, on

the basis of the electronic structure of $Ba_4Ga_4SnSe_{12}$, its direct band gap is mainly determined by the $[Ga_4SnSe_{12}]^{8-}$ anionic framework.

Acknowledgments

This research was supported by National Natural Science Foundation of China (No. 51472251, 21271178, 11274367, and 51402270), Science and Technology Innovation Foundation of Institute of Chemical Materials, China Academy of Engineering Physics (KJCX–201308).

References

- 1 H. Li, C. D. Malliakas, Z. Liu, J. A. Peters, H. Jin, C. D Morris, L. Zhao, B. W. Wessels, A. J. Freeman and M. G. Kanatzidis, *Chem. Mater.*, 2012, **24**, 4434.
- 2 D. Y. Chung, T. Hogan, P. Brazis, M. Rocci-Lane, C. Kannewurf, M. Bastea, C. Uher and M. G. Kanatzidis, *Science*, 2000, **287**, 1024.
- 3 K. Mitchell, F. Q. Huang, A. D. McFarland, C. L. Haynes, R. C. Somers, R. P. Van Duyne and J. A. Ibers, *Inorg. Chem.*, 2003, 42, 4109.
- 4 K. Mitchell, C. L. Haynes, A. D. McFarland, R. P. Van Duyne and J. A. Ibers, *Inorg. Chem.*, 2002, 41, 1199.
- J. Yao, B. Deng, L. J. Sherry, A. D. McFarland, D. E. Ellis, R. P. Van Duyne and J. A. Ibers, *Inorg. Chem.*, 2004, 43, 7735.
- 6 K. Mitchell, F. Q. Huang, E. N. Caspi, A. D. McFarland, C. L. Haynes, R. C. Somers, J. D. Jorgensen, R. P. Van Duyne and J. A. Ibers, *Inorg. Chem.*, 2004, 43, 1082.
- 7 G. H. Chan, L. J. Sherry, R. P. Van Duyne and J. A. Ibers, Z. Anorg. Allg. Chem., 2007, 633, 1343.
- 8 D. E. Bugaris and J. A. Ibers, *Inorg. Chem.*, 2012, **51**, 661.
- Chung, J. H. Song, J. I. Jang, A. J. Freeman, J. B. Ketterson and M. G. Kanatzidis,
 J. Am. Chem. Soc., 2009, 131, 2647.
- 10 T. K. Bera, J. I. Jang, J. B. Ketterson and M. G. Kanatzidis, J. Am. Chem. Soc., 2008, 131, 75.
- 11 H. J. Zhao, Y. F. Zhang and L. Chen, J. Am. Chem. Soc., 2012, 134, 1993.

- 12 M. C. Chen, L. H. Li, Y. B. Chen and L. Chen, *J. Am. Chem. Soc.*, 2011, **133**, 4617.
- 13 T. K. Bera, J. H. Song, A. J. Freeman, J. I. Jang, J. B. Ketterson and M. G. Kanatzidis, *Angew. Chem. Int. Edit.*, 2008, 47, 7828.
- 14 T. K. Bera, J. I. Jang, J. H. Song, C. D. Malliakas, A. J. Freeman, J. B. Ketterson and M. G. Kanatzidis, *J. Am. Chem. Soc.*, 2010, **132**, 3484.
- 15 L. Shi, P. Yin, H. Zhu and Q. Li, *Langmuir*, 2013, **29**, 8713.
- 16 L. Shi, C. Pei, Y. Xu and Q. Li, J. Am. Chem. Soc., 2011, 133, 10328.
- 17 L. Shi and Q. Li, CrystEngComm, 2011, 13, 6507.
- 18 M. C. Chen, L. M. Wu, H. Lin, L. J. Zhou and L. Chen, J. Am. Chem. Soc., 2012, 134, 6058.
- 19 Y. K. Chen, M. C. Chen, L. J. Zhou, L. Chen and L. M. Wu, *Inorg. Chem.*, 2013, 52, 8334.
- 20 W. Yin,; D. Mei,; J. Yao,; P. Fu,; Y. Wu, J. Solid State Chem., 2010, 183, 2544.
- 21 H. J. Zhao, L. H. Li, L. M. Wu and L. Chen, *Inorg. Chem.*, 2009, 48, 11518.
- 22 T. K. Bera and M. G. Kanatzidis, *Inorg. Chem.*, 2012, **51**, 4293.
- 23 T. Van Almsick and W. S. Sheldrick, Z. Anorg. Allg. Chem., 2005, **631**, 1746.
- 24 H. J. Zhao, L. H. Li, L. M. Wu and L. Chen, *Inorg. Chem.*, 2010, **49**, 5811.
- 25 L. Geng, W. D. Cheng, C. S. Lin, W. L. Zhang, H. Zhang and Z. Z. He, *Inorg. Chem.*, 2011, 50, 5679.
- 26 Y. Wu and W. Bensch, *Inorg. Chem.*, 2009, 48, 2729.
- 27 W. Hao, D. Mei, W. Yin, K. Feng, J. Yao and Y. Wu, J. Solid State Chem., 2013,

198, 81.

- 28 W. Yin, K. Feng, W. Wang, Y. Shi, W. Hao, J. Yao and Y. Wu, *Inorg. Chem.*, 2012, 51, 6860.
- 29 W. Yin, W. Wang, L. Bai, K. Feng, Y. Shi, W. Hao, J. Yao and Y. Wu, *Inorg. Chem.*, 2012, **51**, 11736.
- 30 Z. Z. Luo, C. S. Lin, W. L. Zhang, H. Zhang, Z. Z. He and W. D. Cheng, *Chem. Mater.*, 2013, 26, 1093.
- 31 Z. Z. Luo, C. S. Lin, H. H. Cui, W. L. Zhang, H. Zhang, Z. Z. He and W. D. Cheng, *Chem. Mater.*, 2014, **26**, 2743.
- 32 K. Feng, X. Zhang, W. Yin, Y. Shi, J. Yao and Y. Wu, *Inorg. Chem.*, 2014, **53**, 2248.
- 33 C. Y. Meng, H. Chen, P. Wang and L. Chen, *Chem. Mater.*, 2011, **23**, 4910.
- 34 A. Mesbah, S. Lebegue, J. M. Klingsporn, W. Stojko, R. P. Van Duyne and J. A. Ibers, *J. Solid State Chem.*, 2013, **200**, 349.
- 35 J. Baboa and T. E. Albrecht-Schmitt, J. Solid State Chem., 2013, 197, 414.
- 36 B. W. Rudyk, S. S. Stoyko and A. Mar, J. Solid State Chem., 2013, 208, 78.
- 37 W. Yin, K. Feng, R. He, D. Mei, Z. Lin, J. Yao and Y. Wu, *Dalton Trans.*, 2012, **41**, 5653.
- 38 K. Feng, X. Jiang, L. Kang, W. Yin, W. Hao, Z. Lin, J. Yao, Y. Wu and C. Chen, *Dalton Trans.*, 2013, **42**, 13635.
- 39 CrystalClear. Rigaku Corporation, Tokyo, Japan 2008.
- 40 G. M. Sheldrick, Acta Crystallogr., Sect. A, 2008, 64, 112.

- 41 M. C. Payne, M. P. Teter, D. C. Allan, T. A. Arias and J. D. Joannopoulos, *Rev. Mod. Phys.*, 1992, **64**, 1045.
- 42 S. J. Clark, M. D. Segall, C. J. Pickard, P. J. Hasnip, M. J. Probert, K. Refson and M. C. Payne, Z. Kristallogr., 2005, 220, 567.
- 43 W. Kohn, Rev. Mod. Phys., 1999, 71, 1253.
- 44 D. M. Ceperley and B. J. Alder, *Phys. Rev. Lett.*, 1980, **45**, 566.
- 45 J. S. Lin, A. Qteish, M. C. Payne and V. Heine, *Phys. Rev. B*, 1993, **47**, 4174.
- 46 H. J. Monkhorst and J. D. Pack, *Phys. Rev. B*, 1976, **13**, 5188.
- 47 W. Yin, D. Mei, K. Feng, J. Yao, P. Fu and Y. Wu, *Dalton Trans.*, 2011, 40, 9159.
- 48 W. Yin, K. Feng, D. Mei, J. Yao, P. Fu and Y. Wu, Dalton Trans., 2012, 41, 2272.
- 49 I. D. Brown and D. Altermatt, *Acta Crystallogr., Sect. B: Struct. Sci.*, 1985, **41**, 244–247.
- 50 J. Yao, D. Mei, L. Bai, Z. Lin, W. Yin, P. Fu and Y. Wu, *Inorg. Chem.*, 2010, 49, 9212.
- 51 A. Assoud and H. Kleinke, *Solid State Sci.*, 2010, **12**, 919.
- 52 W. Klee and H. Schäfer, Z. Anorg. Allg. Chem., 1981, 479, 125.
- 53 D. Mei, W. Yin, Z. Lin, R. He, J. Yao, P. Fu and Y. Wu, J. Alloys Compd., 2011, 509, 2981.
- 54 K. Dobletov, Y. A. Markhuda, A. V. Anikin and A. Ashirov, *Inorg. Mater.*, 1978, **14**, 24.
- 55 O. Schevciw and W. B. White, *Mater. Res. Bull.*, 1983, **18**, 1059.
- 56 M. H. Lee, C. H. Yang and J. H. Jan, *Phys. Rev. B*, 2004, **70**, 235110(1).

Figure Captions

- Fig. 1 The SEM picture of as-grown Ba₄Ga₄SnSe₁₂ crystal.
- Fig. 2 The SEM picture of as-grown Ba₆Ga₂SnSe₁₁ crystal.
- **Fig. 3** Powder X–ray diffraction pattern of Ba₄Ga₄SnSe₁₂ and the simulated pattern based on the single crystal crystallographic data.
- **Fig. 4** Powder X–ray diffraction pattern of Ba₆Ga₂SnSe₁₁ and the simulated pattern based on the single crystal crystallographic data.
- **Fig. 5** Unit cell of the Ba₄Ga₄SnSe₁₂ structure viewed along [001].
- **Fig. 6** The $[Ga_2SnSe_{10}]^{10^-}$ layer in $Ba_4Ga_4SnSe_{12}$ viewed along [110].
- Fig. 7 The [Li₂GaSe₆]⁷⁻ layer in Ba₄Ga₅LiSe₁₂ viewed along [110].
- Fig. 8 Unit cell of the Ba₆Ga₂SnSe₁₁ structure viewed along [001].
- Fig. 9 Diffuse reflectance spectra of Ba₄Ga₄SnSe₁₂ and Ba₆Ga₂SnSe₁₁.
- **Fig. 10** The electronic band structure (a) and total/partial density of states (DOS/PDOS) (b) in the Ba₄SnGa₄Se₁₂ crystal.

Table 1 Crystal Data and Structure Refinements for Ba₄Ga₄SnSe₁₂ and Ba₆Ga₂SnSe₁₁

	Ba ₄ Ga ₄ SnSe ₁₂	Ba ₆ Ga ₂ SnSe ₁₁
fw	1894.45	1950.73
a(Å)	13.607(2)	18.715(4)
b(Å)	13.607(2)	7.109(1)
c(Å)	6.510(1)	19.165(4)
β(°)	90.00	103.29(3)
$V(Å^3)$	1205.2(3)	2481.5(8)
Space group	$P\overline{4}2_1/c$	<i>P</i> 2 ₁ / <i>c</i>
Z	2	4
$\rho_c(g/cm^3)$	5.221	5.221
μ (cm ⁻¹)	29.943	28.598
$R(F)^a$	0.0465	0.0516
$R_{\rm W}(F_{\rm o}^2)^b$	0.1056	0.1103
z^b	0.04	0.04

 $^{{}^{}a}R(F) = \sum ||F_{o}| - |F_{c}|| / \sum |F_{o}| \text{ for } F_{o}^{2} > 2\sigma(F_{o}^{2}).$

 $^{{}^{}b}R_{w}(F_{o}^{2}) = \{\sum [w(F_{o}^{2}-F_{c}^{2})^{2}] / \sum wF_{o}^{4}\}^{\frac{1}{2}} \text{ for all data. } w^{-1} = \sigma^{2}(F_{o}^{2}) + (zP)^{2}, \text{ where } P$ $= (\text{Max}(F_{o}^{2}, 0) + 2F_{c}^{2})/3.$

Table 2 Selected Interatomic Distances (Å) for Ba₄Ga₄SnSe₁₂

$Ba_{4}Ga_{4}SnSe_{12} \\$				
Bond	Distance	Bond	Distance	
Ba-Se3	3.295(1)	Ba-Se1	3.658(1)	
Ba-Se2	3.340(1)	Ga-Se3	2.387(2)	
Ba-Se3	3.352(1)	Ga-Se1	2.402(2)	
Ba-Se3	3.361(2)	Ga-Se2	2.419(2)	
Ba-Se1	3.379(1)	Ga-Se2	2.451(2)	
Ba-Se2	3.393(1)	Sn-Se1×4	2.438(1)	
Ba-Se3	3.401(2)			

Table 3 Selected Interatomic Distances (Å) for Ba₆Ga₂SnSe₁₁

$Ba_{6}Ga_{2}SnSe_{11} \\$					
Bond	Distance	Bond	Distance	Bond	Distance
Ba1-Se7	3.166(1)	Ba3-Se8	3.507(1)	Ba6-Se4	3.449(1)
Ba1-Se11	3.250(1)	Ba3-Se9	3.719(1)	Ba6-Se5	3.490(1)
Ba1-Se8	3.325(1)	Ba3-Se9	3.721(1)	Ba6-Se8	3.572(1)
Ba1-Se4	3.471(1)	Ba4-Se7	3.220(2)	Ba6-Se8	3.582(1)
Ba1-Se2	3.498(1)	Ba4-Se9	3.294(2)	Sn1-Se9	2.497(1)
Ba1-Se5	3.550(1)	Ba4-Se5	3.337(1)	Sn1-Se11	2.514(1)
Ba1-Se2	3.627(1)	Ba4-Se11	3.374(1)	Sn1-Se2	2.536(1)
Ba1-Se2	3.648(1)	Ba4-Se4	3.383(1)	Sn1-Se7	2.549(2)
Ba2-Se8	3.266(1)	Ba4-Se2	3.404(1)	Sn1A-Se9	2.479(5)
Ba2-Se6	3.343(1)	Ba4-Se11	3.551(1)	Sn1A-Se11	2.502(6)
Ba2-Se3	3.363(1)	Ba4-Se11	3.775(1)	Sn1A-Se2	2.578(5)
Ba2-Se3	3.416(1)	Ba5-Se3	3.209(1)	Sn1A-Se7	2.968(7)
Ba2-Se6	3.418(1)	Ba5-Se6	3.212(1)	Ga1-Se5	2.358(1)
Ba2-Se1	3.487(1)	Ba5-Se5	3.262(1)	Ga1-Se4	2.368(1)
Ba2-Se10	3.655(1)	Ba5-Se4	3.284(1)	Ga1-Se8	2.400(1)
Ba2-Se10	3.724(1)	Ba5-Se10	3.324(1)	Ga1-Se1	2.466(1)
Ba2-Se10	3.746(1)	Ba5-Se1	3.414(1)	Ga2-Se3	2.367(1)

Ba3-Se7	3.243(1)	Ba5-Se1	3.714(1)	Ga2-Se6	2.368(1)
Ba3-Se6	3.293(1)	Ba5-Se1	3.752(1)	Ga2-Se10	2.381(1)
Ba3-Se3	3.316(1)	Ba6-Se10	3.110(1)	Ga2-Se1	2.496(1)
Ba3-Se4	3.454(1)	Ba6-Se9	3.271(1)		
Ba3-Se5	3.454(1)	Ba6-Se2	3.366(1)		

 $\label{eq:table 4} \textbf{Table 4} \mbox{ The calculated band valence sums (BVS) for Ba, Ga, and Sn atoms in $$Ba_4Ga_4SnSe_{12}$ and $Ba_6Ga_2SnSe_1$$}$

Ba ₄ Ga ₄ SnSe ₁₂				
Atom	BVS	Atom	BVS	
Ba	2.043	Ga	2.939	
Sn	4.860			
$Ba_6Ga_2SnSe_{11}$				
Atom	BVS	Atom	BVS	
Bal	2.014	Ba2	1.964	
Ba3	1.892	Ba4	2.107	
Ba5	2.330	Ba6	1.934	
Gal	3.133	Ga2	3.102	
Sn1	4.043	Sn1A	3.387	

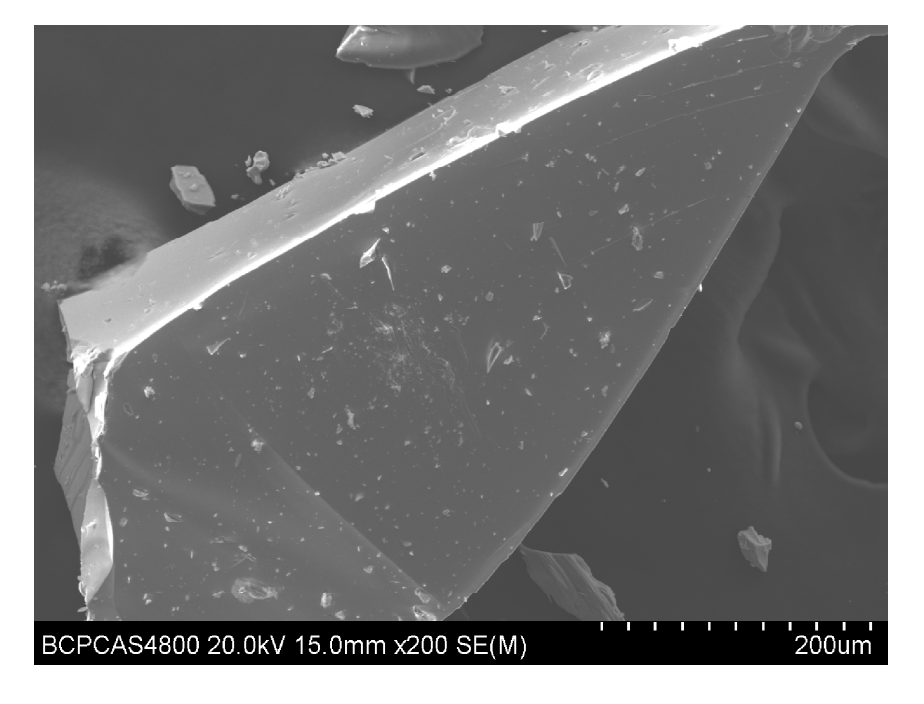


Fig. 1 The SEM picture of as-grown Ba₄Ga₄SnSe₁₂ crystal.

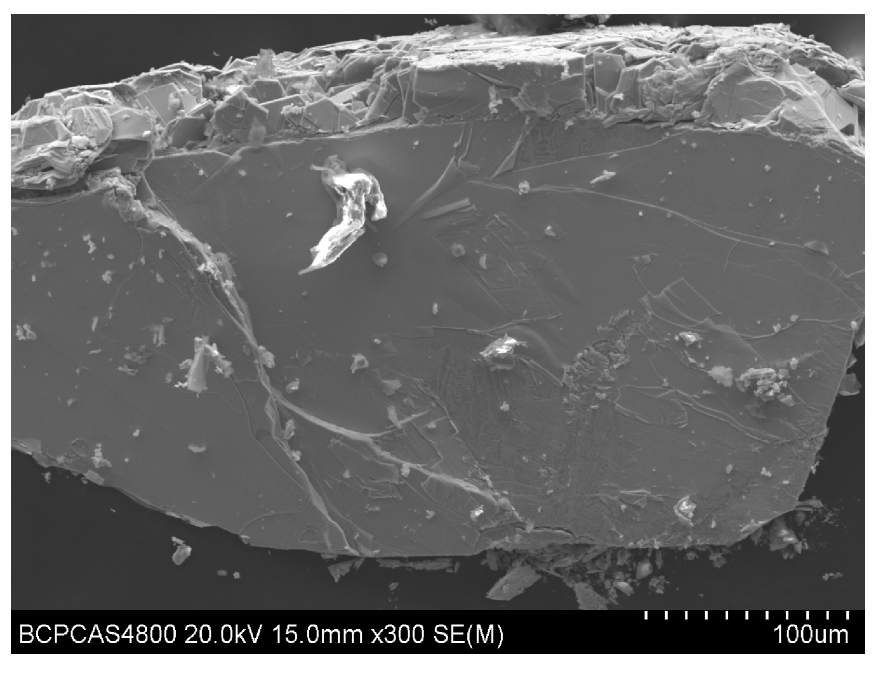


Fig. 2 The SEM picture of as—grown Ba₆Ga₂SnSe₁₁ crystal.

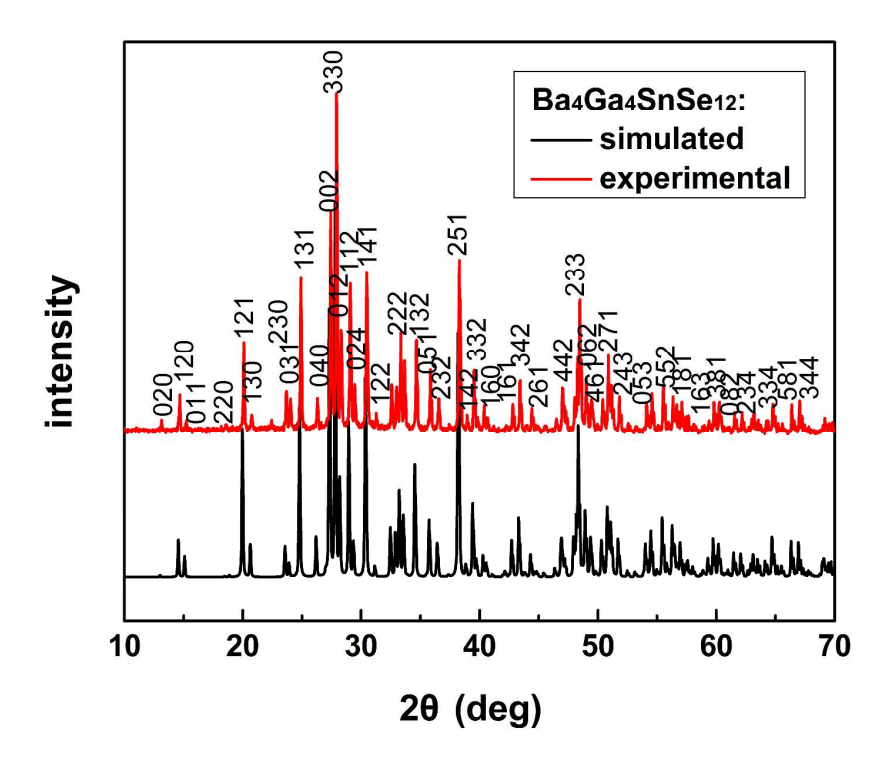


Fig. 3 Powder X-ray diffraction pattern of Ba₄Ga₄SnSe₁₂ and the simulated pattern based on the single crystal crystallographic data.

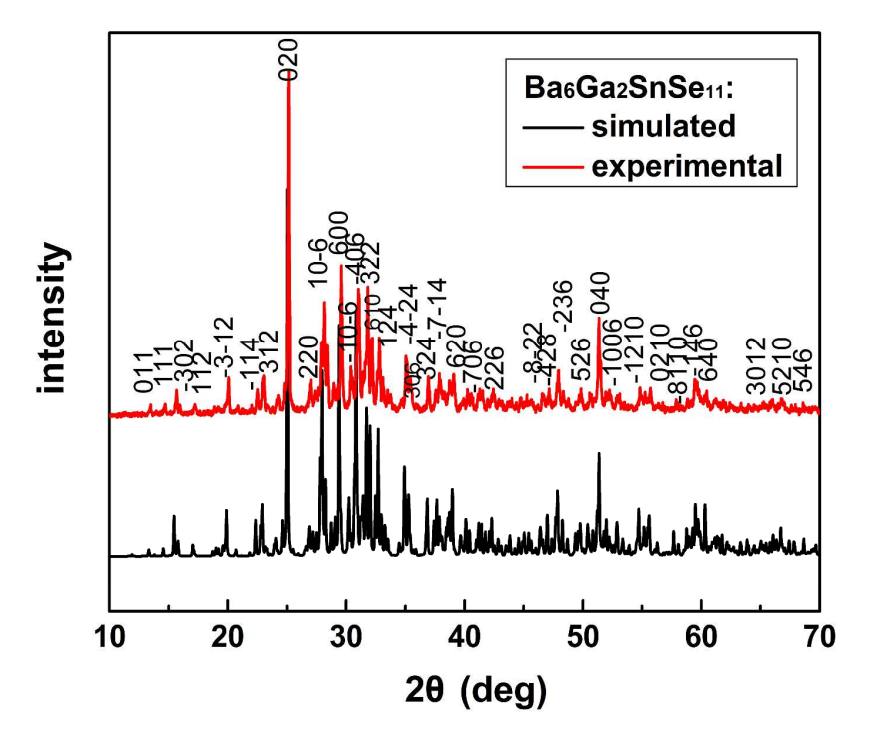


Fig. 4 Powder X-ray diffraction pattern of Ba₆Ga₂SnSe₁₁ and the simulated pattern based on the single crystal crystallographic data.

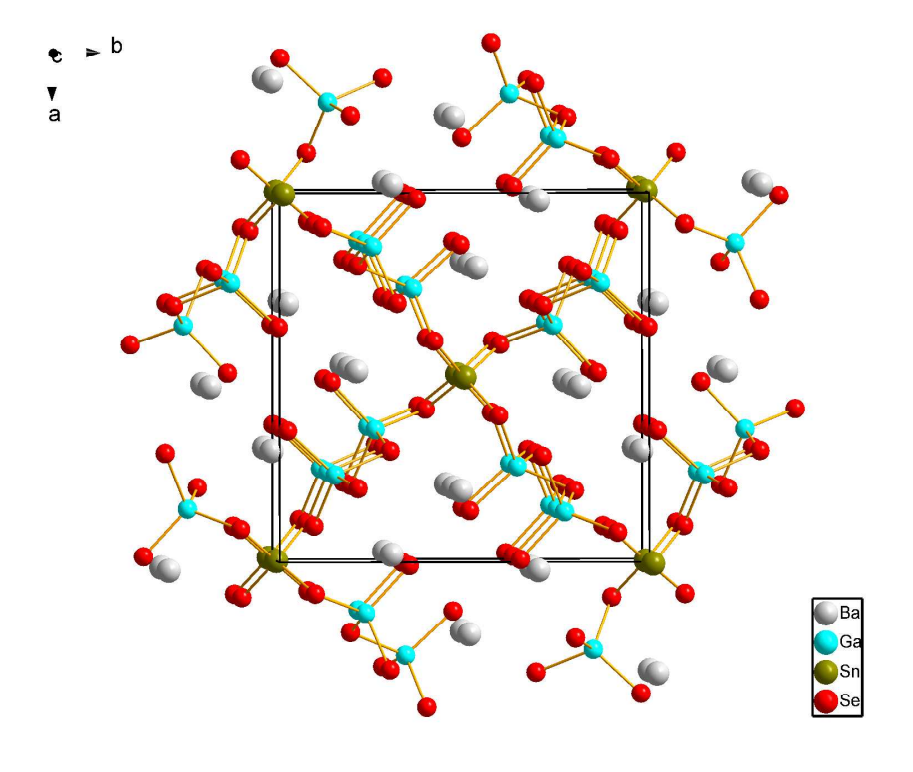


Fig. 5 Unit cell of the Ba₄Ga₄SnSe₁₂ structure viewed along [001].

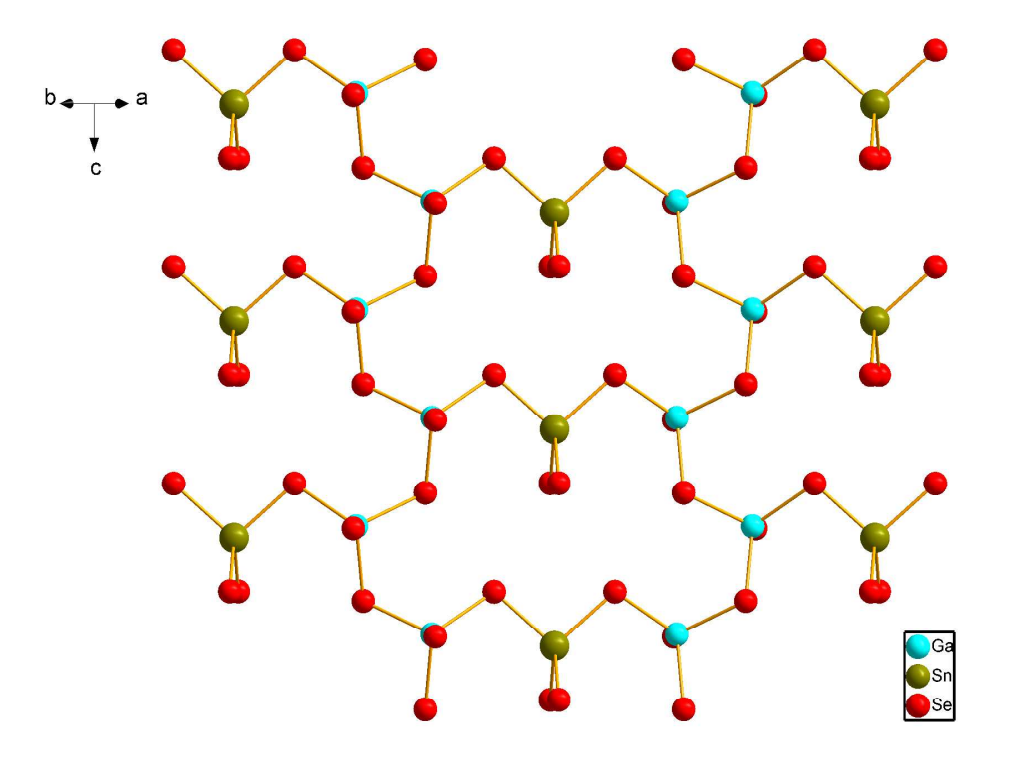


Fig. 6 The $[Ga_2SnSe_{10}]^{10-}$ layer in $Ba_4Ga_4SnSe_{12}$ viewed along [110].

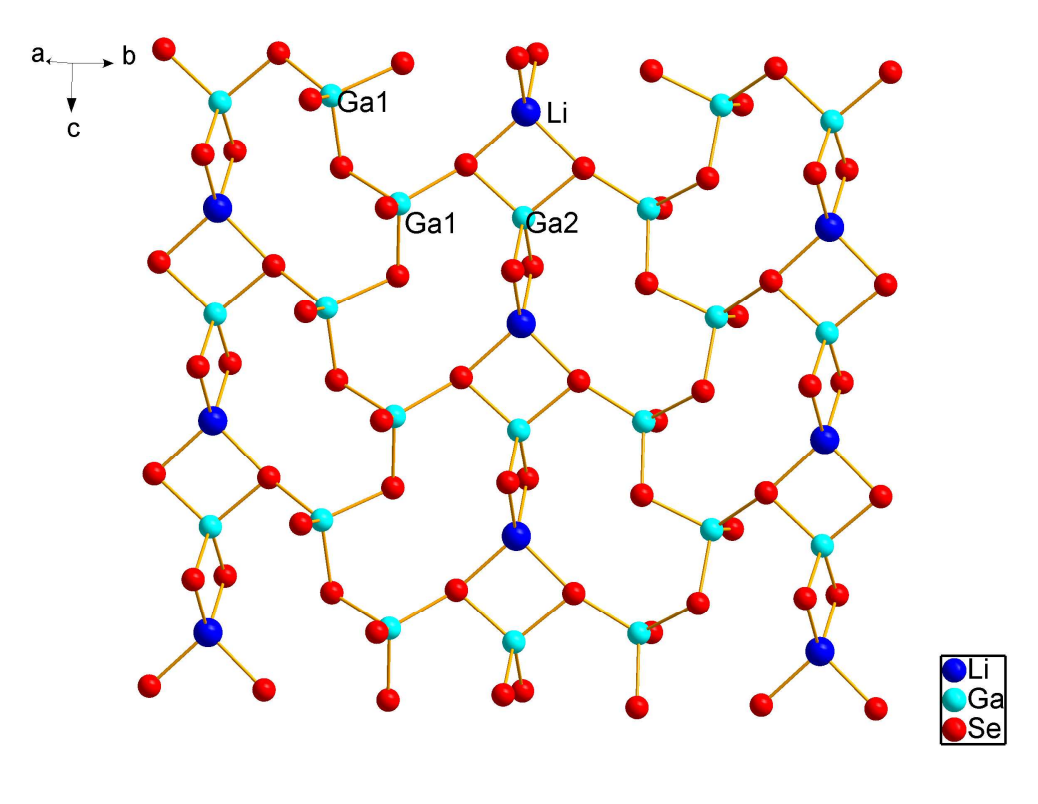


Fig. 7 The $[Li_2GaSe_6]^{7-}$ layer in $Ba_4Ga_5LiSe_{12}$ viewed along [110].

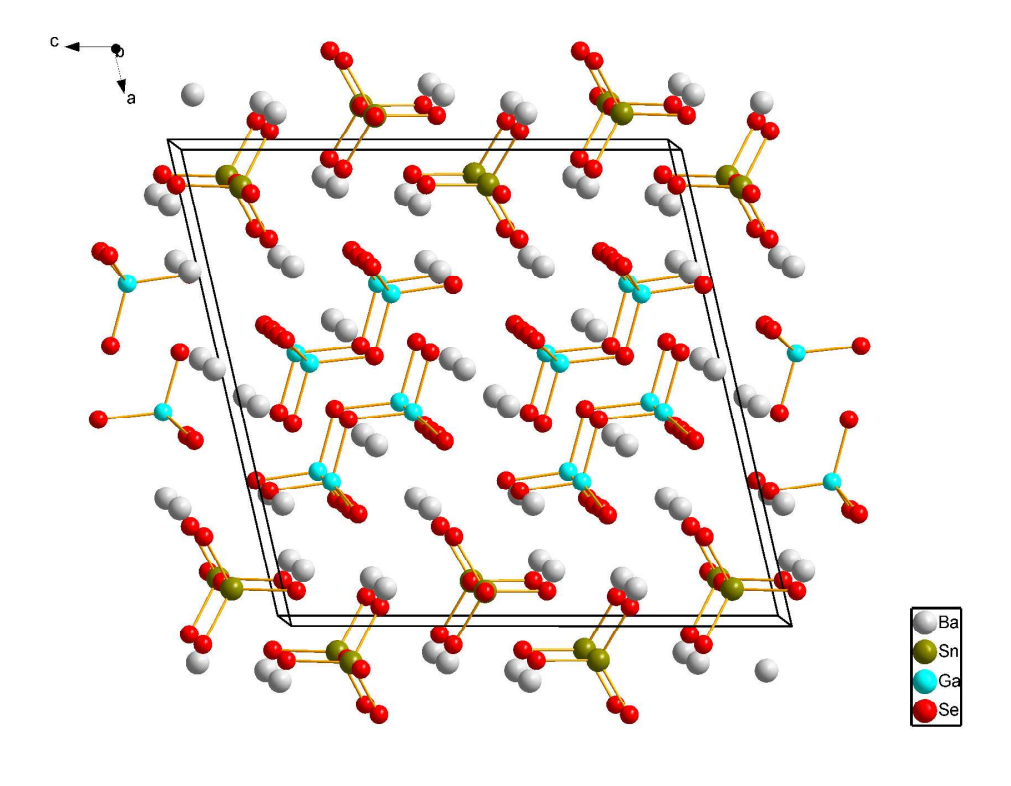


Fig. 8 Unit cell of the Ba₆Ga₂SnSe₁₁ structure viewed along [001].

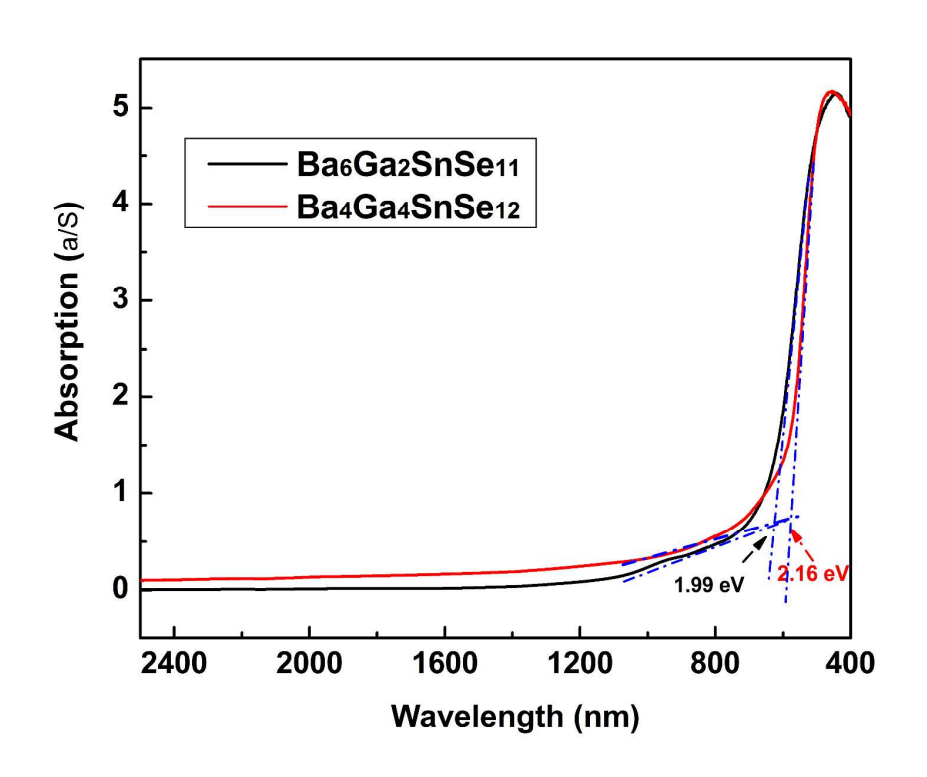


Fig. 9 Diffuse reflectance spectra of Ba₄Ga₄SnSe₁₂ and Ba₆Ga₂SnSe₁₁.

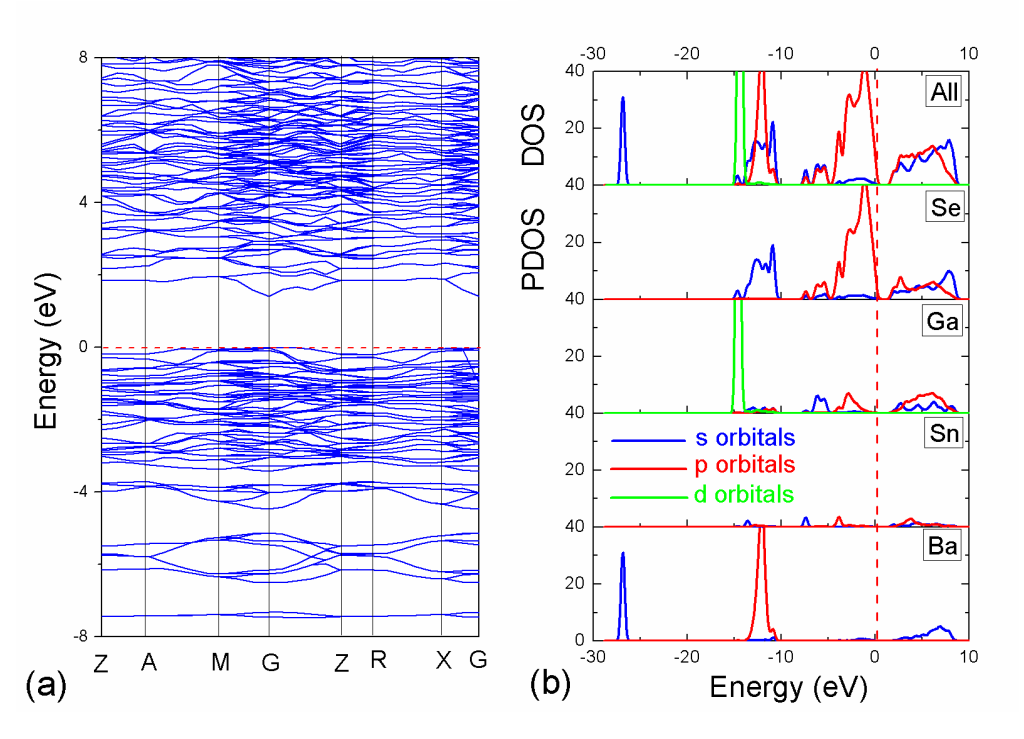


Fig. 10 The electronic band structure (a) and total/partial density of states (DOS/PDOS) (b) in the $Ba_4SnGa_4Se_{12}$ crystal.

Graphical Abstract

Two new quaternary selenides $Ba_4Ga_4SnSe_{12}$ and $Ba_6Ga_2SnSe_{11}$, representing the first two members in the A/M/Sn/Q (A = alkaline–earth metal; M = Al, Ga, In; Q = S, Se, Te) system, have been synthesized. $Ba_4Ga_4SnSe_{12}$ has a three–dimensional structure built up from corner–sharing $GaSe_4$ and $SnSe_4$ tetrahedra with Ba^{2+} cations residing in the cavities. $Ba_6Ga_2SnSe_{11}$ features a zero–dimensional structure containing totally isolated distorted $SnSe_4$ tetrahedra and discrete Ga_2Se_7 unit with Ba^{2+} cations located between them. The band gaps are 2.16 (2) eV and 1.99 (2) eV for $Ba_4Ga_4SnSe_{12}$ and $Ba_6Ga_2SnSe_{11}$ respectively. The electronic structure calculation indicates that $Ba_4Ga_4SnSe_{12}$ is a direct–gap semiconductor with the band gap mainly determined by the $[Ga_4SnSe_{12}]^{8-}$ anionic framework.

